Technical University of Liberec
Faculty of Mechatronics, Informatics and Interdisciplinary Studies
Institute of Novel Technologies and Applied Informatics

An Investigation of Aggregation Models of Magnetic, Zero-valent Iron Nanoparticles

Model agregace magnetických nanočástic nulmocného železa

by

Dana Rosická

supervisor: doc. Ing. Jan Šembera, Ph.D.

A thesis statement submitted in partial fulfilment for the degree of Doctor abbreviated to Ph.D.

Study Programme: P3901 / Applied sciences in engineering
Study field: 3901V025 / Science Engineering

June 2013

Technical University of Liberec
Faculty of Mechatronics, Informatics and Interdisciplinary Studies

ABSTRACT

This work focuses on an investigation into the aggregation mechanisms of unstable, nanoscale particles in flowing groundwater. A study and a description of the process of aggregation help to simulate the transport of unstable undissolved nanoparticles. This could be useful when one needs to know how the nanoparticles behave in transit. In the following example a knowledge of this process is helpful. Some contaminants, such as halogenated hydrocarbons, are remediable by zero-valent iron nanoparticles. These are very unstable particles but still have a high potential in remediation field. Thanks to their (nano)size, they can migrate through the ground and are able to decontaminate wide areas. However, they aggregate into microsized entities and lose their migratory ability. Simulation of the transport of iron nanoparticles and their aggregation could be useful in predicting the success of decontamination interventions. The mathematical derivation of iron nanoparticle aggregation is so complex and difficult that this work is focused mainly on them.

This work is mainly theoretical. First, an aggregation model is described. The model is based on aggregation due to the heat fluctuation of nanoparticles and due to their different velocities during sedimentation and drifting in groundwater. This model is then extended to include the impact of repulsive electrostatic and attractive magnetic forces that affect the rate of aggregation of magnetic nanoparticles with non-zero surface charge. The coefficients of aggregation are recalculated in order to compute the aggregation not only between single nanoparticles, but also between aggregates of nanoparticles (more simply called "particles"). A study of the possible aggregate structures was performed to be able to compute their mutual reactions. Extended coefficients of aggregation between particles were converted to coefficients of aggregation between "sections" of nanoparticles with similar size and properties. This enabled the simulation of aggregation in real time. The subsequent part of this work is dedicated to the computational aspects of aggregation in order to make the computation faster, but with a small error. At the end of the work, simulations of bentonite and iron nanoparticle aggregation and transport in the ground are presented.

Technická univerzita v Liberci
Fakulta mechatroniky, informatiky a mezioborových studií

ABSTRAKT

Tato práce se zabývá procesem agregace nestabilních nanočástic s nenulovým povrchovým nábojem a magnetizací, unášených vodou. Motivací pro tuto práci byla potřeba simulovat transport zejména následujícího typu nestabilních nanočástic. Pro sanační účely jsou používány nulmocné železné nanočástice. Jde o velmi reaktivní nanočástice s velkým měrným povrchem schopné dekontaminovat například halogenové uhlovodíky. Nančástice však zároveň ve velké míře agregují, což vede k omezení migračních schopností nanočástic. I přes to jde o velmi ceněné sanační činidlo. Porozumění agregaci železných nanočástic může být užitečné pro simulaci jejich transportu potažmo pro odhad účinnosti sanačního zásahu. Odvození agregace těchto částic je velmi komplexní a komplikovaný problém, proto je tato práce zaměřena zejména na ně.

Tato práce je především teoretická. Nejprve je zde popsán obecný model agregace založený na Brownově pohybu a na různých rychlostech částic při sedimentaci a migraci v proudu vody. Tento model je zde rozšířen o vliv odpudivých elektrostatických sil a přitažlivých magnetických sil. Koeficienty určující agregaci jsou přeformulovány tak, aby byla počítána agregace nejen mezi jednotlivými nanočásticemi, ale také mezi agregáty nanočástic. Zároveň jsou zde zkoumány struktury, které nanočástice v agregátech nejpravděpodobněji zaujímají. Pro všechny další výpočty je pak vybrána jedna struktura agregátů. Z důvodu výpočetní náročnosti agregace mezi všemi různě velkými agregáty je zde představen model klastrování, kdy částice (agregáty) jsou rozděleny do klastrů podle velikosti a agregace je počítána pomocí reakcí mezi těmito klastry. Ze stejného důvodu je dále zkoumána možnost zrychlení výpočtů agregace průměrováním agregátů. Na závěr jsou představeny některé simulace transportu nanočástic a jejich agregace.

Contents

Chapter 1

Introduction

1.1 Problem Statement

Many types of nanoparticles and colloidal particles occur in groundwater. Some of the particles are formed naturally; others are generated synthetically and put into the ground by human activity. It may be necessary to know both the reactivity of the nanoparticles in the ground and their migratory properties for simulation of their behaviour in the ground. That is the reason why the processes of mutual nanoparticle reactions (aggregation) during their transport through the ground are examined in the thesis. Studies of the problem of particle aggregation have been published before [1–3], but are insufficient for a description of the interactions between nanoparticles with non-zero surface charge and/or magnetic moment. These types of nanoparticles are examined at the Technical University of Liberec (TUL) where experiments and simulations of nanoscale zero-valent iron (nZVI) reactivity and transport are performed. nZVI describes iron nanoparticles used for water and soil treatment. They are able to migrate in groundwater through contaminated areas and remediate polluted soils and water [4]. The properties of nZVI depend on their production method which can be carried out in many ways [5–7]. The thesis mainly deals with RNIP and NANOFER nZVI described in Section 2. However, the derived models in the thesis are general and can be used for the computation of aggregation of migrating nanoparticles with/without magnetic and/or electrostatic mutual interactions.

1.2 Motivation and Challenges

To be able to simulate the migration of magnetic nanoparticles with non-zero surface charge a knowledge of how they behave during migration was required. A lot of experiments concerning nZVI transport through a porous medium have been performed at

TUL [8] (in Czech language (CL)). Hence, it was possible to describe the mutual interactions between nZVI nanoparticles and to verify the new model of aggregation on the results of the transport experiments. The basis was an aggregation model of unstable nanoparticles derived from these articles: [1–3], and specified in the author's diploma thesis [9](CL). The aim was to include the effects of electrostatic and magnetic forces on the old aggregation model and make the model more general. The old commonly used aggregation model with mass transport coefficients [3,10] describing aggregation is based on collisions between nanoparticles caused by heat fluctuation and the different velocities of nanoparticles during settlement and drifting. This model does not include a reduction in the aggregation rate due to repulsive electrostatic forces which themselves occur due to the electric double-layer which forms on the nanoparticle surfaces [11]. Furthermore, in the case of magnetic nanoparticles, the aggregation is rapidly accelerated by attractive magnetic forces between nanoparticles [5, 12–15]. Therefore the aggregation model had to be extended and a more accurate model of aggregation of iron nanoparticles in water could be achieved.

1.3 Contributions

The main contribution of this work is that it enables the computation of aggregation dynamics of general nanoparticles where the effect of electrostatic and magnetic forces can be included. This was achieved by carrying out the following actions.

- The mass transport coefficients (MTC) were extended to include the impact of repulsive electrostatic forces and attractive magnetic forces between particles. Mass transport coefficients give the frequency of collisions between nanoparticles or aggregates of nanoparticles (particles). Magnetic forces were added by creating a "limit distance" which gives the critical distance between aggregates in which magnetic forces attract particles and cause aggregation.
- The probable structures of aggregates created from nanoparticles were assessed. The effect of magnetic forces on the aggregation rate of some probable structures was computed and a comparison was made of the experimental results. Next, the interaction energies between nanoparticles in aggregates were computed. These are the interactions which produce the most stable structures of aggregates of magnetic nanoparticles.
- Computation of all reactions between every single nanoparticle and aggregate is very time-consuming. Therefore, a system of clustering the particles into "sections" with similar properties according to their sizes was derived based on the work: [16]. The aggregation model was then adapted to compute the reactions between the particle size sections (PSS). That accelerated the computation of the

mass transport coefficient and enabled the transformation of the mass transport coefficient into kinetic reactions between sections of particles. That enabled the new aggregation model to be used in a variety of simulation software.

- The possibility of averaging the PSS and their acting forces was examined in order to accelerate the aggregation computation. The influence of averaging the magnetic force computation on computational error was analyzed and when it is suitable to use the averaging model was assessed.

- The extended aggregation model of iron nanoparticles was converted into a kinetic form of the aggregation between PSS and included into a formula for particle transport in groundwater. This can be used to simulate the transport of iron nanoparticles and to predict the efficiency of a remedial intervention. That could be useful when proposing an optimal remedial intervention which would enable the decontamination of an affected area efficiently and economically.

Parts of this work were developed within the following projects: "Advanced Remediation Technologies and Processes Centre" 1M0554 - Programme of Research Centres PP2-DP01, "Non-standard application of physical fields analogy, modelling, verification and simulation" no. 102/08/H081, project no. 7822 of the Technical University in Liberec, the research project FR-TI1/456 "Development and implementation of the tools additively modulating soil and water bioremediation" and the research project FRTI1/362.

The work in the thesis has been published in part or in full in the following publications:

Journal:

- Rosická D., Šembera J.: Changes in the nanoparticle aggregation rate due to the additional effect of electrostatic and magnetic forces on mass transport coefficients, Nanoscale Res. Lett. 2013, 8(20).

- Rosická D., Šembera J.: Influence of structure of iron nanoparticles in aggregates on their magnetic properties, Nanoscale Res. Lett. 2011, 6(527).

- Szilágyi I., Rosická D., Hierrezuelo J., Borkovec M.: Charging and stability of anionic latex particles in the presence of linear poly(ethylene imine), J. Colloid Interface Sci. 2011, 360(2):580-5.

- Šembera J., Rosická D.: Computational Methods for Assessment of Magnetic Forces Between Iron Nanoparticles and Their Influence on Aggregation, Adv. Sci. Eng. Med. 2011, 3(1-2):149-154(6).

- Rosická D., Šembera J.: Assessment of Influence of Magnetic Forces on Aggregation of Zero-valent Iron Nanoparticles, Nanoscale Res Lett 2011, 6(10).

Conference:

- Rosická D., Šembera J.: Method of simulation of magnetic nanoparticle aggregation with using clustering system, 4th International Conference NANOCON 2012, Brno 2012 (October 23rd - 25th 2012), Conference Proceedings Book, in print.
- Rosická D., Šembera J.: Inclusion of Electrostatic Forces to Assessment of Rate of Magnetic Forces Impact to Iron Nanoparticle Aggregation, 3th International Conference NANOCON 2011 in Olomouc (September 21st-23rd 2011), Conference Proceedings Book (ISBN 978-80-87294-27-7), 387–392.
- Rosická D., Šembera J., Maryška J.: Theoretical study of electrical charge influence on aggregation rate of zero valent iron, 18th Annual International Conference on Composites/Nano Engineering (ICCE -18) 2010 in Anchorage, Alaska (July 4-10, 2010), Book of Abstracts, 641–642.

1.4 Outline of the Thesis

This prelude has introduced the idea of deriving an aggregation model of nanoparticles with non-zero surface charge and magnetic moment.

Chapter 2 provides a basic understanding of zero-valent iron nanoparticles (nZVI). The properties of nZVI are listed as well as statistics that support the assumption that the particles are ferromagnetic. The main result in this chapter concerns their high reactivity and rapid aggregation rate.

Chapter 3 describes the aggregation model based on Brownian motion and different velocities of particles during sedimentation and drifting in groundwater. There is a comparison of the importance of these processes on the rate of aggregation for different types of interacting particles (the word “particle” includes both nanoparticles and aggregates).

Chapter 4 presents the impact of including electrostatic forces into the aggregation model from Chapter 3. Electrostatic forces between particles occur because of the electric double-layer that forms around a particle in an electrolyte. The electrostatic forces are added into the mass transport coefficient calculations giving the frequency of collisions between particles. Measurement of the zeta-potential of nZVI depending on the pH of the solution is also presented here. The surface charge is quantifiable from the measured zeta-potential. The effect of including the surface charge in the model of the aggregation rate is considered at the end of this chapter.

Chapter 5 is concerned with a sectional model of the computation of aggregation between particles. The aggregation can be viewed as first-order kinetic reactions when two

particles collide and result in one particle. A huge number of reactions would have to be computed to describe an aggregation between every different nanoparticle and aggregate. Therefore, the particles are categorized into "sections" according to their size. The reactions between these sections are calculated instead of between the individual particles. Modified mass transport coefficients for this computation are defined in this chapter. Using these modified mass transport coefficients, a time variation in particle size sections (PSS) can be computed and the dynamics of particle aggregation over time can be seen. The computation was very time-consuming so an average was taken of the mass transport coefficients of PSS to compute changes in the number, volume, or surface area of particles in every PSS. The surface area and number of particles change over time but the overall volume of the particles is constant. Computation of the sum of changes in the volume of all the PSS acts as verification of the computation.

Chapter 6 describes the magnetic forces between magnetic iron nanoparticles. First, the magnetic forces between two single nanoparticles are derived, then, the magnetic field around an aggregate of magnetic nanoparticles is examined. The magnetic force between particles strongly depends on the structure that the nanoparticles take in the aggregates. The quantity "Limit distance" is introduced in this chapter. This quantity is an instrument for the estimation of the magnitude of the effect of a magnetic force on the aggregation rate.

Chapter 7 studies the aggregate structures that nanoparticles in the aggregate are likely to take. Unstructured models of aggregates were examined where the positions of nanoparticles are random and also structured models of aggregates where nanoparticles in the aggregates form a pattern or "constellation", such as a chain or a cube, etc. For all the chosen cases the sizes of the magnetic forces were calculated and a decision was made as to whether it was a realistic value or not. Another way of judging a structure of an aggregate that was researched was a computation of the interaction energies between nanoparticles in different constellations of aggregates. The results of the research are summarized in this chapter.

Chapter 8 presents a study of how to accelerate these computations. Computation of the magnetic force between two aggregates is time-consuming because the overall magnetic force is computed as a sum of the magnetic forces between every single nanoparticle from the first aggregate and every single nanoparticle from the second aggregate. A computation of the magnetic force between two "average aggregates" is proposed where the magnetic moment vector of the averaged aggregate is given by the sum of magnetic vectors of all the nanoparticles creating the aggregate. The results generated using the accurate summation method were compared against the faster averaging method. Thus when it is possible to use the averaging method without incurring a large error was estimated.

Chapter 9 provides an overview of computing the limit distance depending not only on the magnetic field around aggregates, but also on the electrostatic field. It is another way of computing the effect of electrostatic forces between particles on the aggregation rate. This way is better when particles are magnetic and have a non-zero surface charge. Repulsive electrostatic forces and attractive magnetic forces act between these particles and the strength of repulsion or attraction depends on the distance between the particles. The limit distance gives a distance from a particle at which the repulsive and attractive forces are equal.

Chapter 10 describes inclusion of the limit distance computation into the mass transport coefficients (MTC) that give the frequency of collisions between particles. Now, the MTCs compute the aggregation rate between particles that oscillate, settle, drift in water, attract each other due to magnetic forces and repulse each other due to their surface charge. A comparison of MTC computations using the old model without the inclusion of electrostatic and magnetic forces and using the new model including the forces is described here.

Chapter 11 is concerned with the conversion of the aggregation model into first-order reactions which are usable in particle transport software. The reactions describe collisions of particles from two sections (either different or the same one) that lead to a single particle formation (that falls into the larger of the two sections or into the section immediately following). Changes in the number of particles in sections leads to a change in particle transport.

Chapter 12 gives some simulations of nanoparticle transport and aggregation in order to verify the theoretical aggregation models. Firstly, the model from Chapter 4 is verified. The model describes the aggregation of nanoparticles caused by their oscillation, different velocities during sedimentation and drifting in water, and their mutual repulsion due to electrostatic forces. Bentonite colloidal nanoparticles were chosen as an example of non-magnetic nanoparticles with non-zero surface charge. Secondly, simulation of migration experiments of one-dimensional nZVI particles were performed. This simulation served to verify the aggregation model with inclusion of both magnetic and electrostatic forces. Thirdly, simulations of a real migration of nZVI in the ground were examined, when the nanoparticles were used for remediation of a real area.

Chapter 13 provides a review of the overall contributions of the thesis and provides some ideas for future work.

Chapter 2

Characterization and properties of nZVI

Zero-valent iron nanoparticles (nZVI) are spherical particles with size in tens and hundreds of nanometers. They have become quite a popular choice for the treatment of hazardous and toxic waste and for the remediation of contaminated sites. nZVI technology is widely used, mainly in North America and Europe [17]. In the U.S. alone, more than 20 projects have been completed since 2001. In Europe, nZVI was first used in the Czech Republic in 2004. Since then, research groups all over the world have been examining nZVI synthesis, reactivity, stabilization, etc.

Many studies have demonstrated the effect of zero-valent iron nanoparticles for the transformation of halogenated organic contaminants and heavy metals [18–21]. In addition, several studies have demonstrated that zero-valent iron is effective in stabilizing or destroying the hosts of pollutants due to its highly reducing character [22]. Therefore, zero-valent iron (ZVI) is used as one of the most reactive materials in permeable reactive barrier (PRB) technology [23]. At nanoscales, ZVI usability extends even further. The specific surface area of nZVI increases dramatically and so the surface reactivity is higher [24]. Laboratory studies have confirmed that nZVI can destroy, stabilize or transform halogenated hydrocarbons, carbon tetrachloride, polychlorinated biphenyls (PCBs), chlorinated organic solvents, organochlorine pesticides and many more pollutants [4, 6, 25–28].

The nZVI are valuable for their high reactivity with pollutants. However, the nZVI particles are very unstable and that leads to rapid aggregation (Fig. 2.1) as a result of attractive magnetic and van der Waals forces [6]. Furthermore, the size and/or surface charge of the aggregates result in a very high deposition on porous media grains, which severely limits its transport in porous media [14, 29].

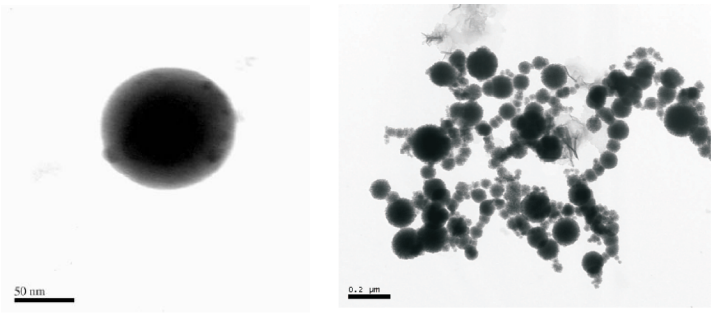

(a) One iron nanoparticle (b) Aggregated nanoparticles

FIGURE 2.1: TEM scan of one iron nanoparticles
Source: [11].

The iron particles corrode in groundwater which causes a change in the surface charge as well as a change in the rate of aggregation of nZVI [30]. In [31], XRD (X-ray diffraction) and SEM results revealed that nZVI gradually converts to magnetite/maghemite corrosion products. The particles have a core-shell structure (Fig. 2.2) where the core is zero-valent iron and the shell consists of iron oxides. This significantly affects the rate of aggregation [5, 12–14]. For simplicity, it was supposed that the iron particle is ferromagnetic in the thesis. In [14], RNIP, that are used in TUL experiments, turned out to behave as single-domain magnetic particles.

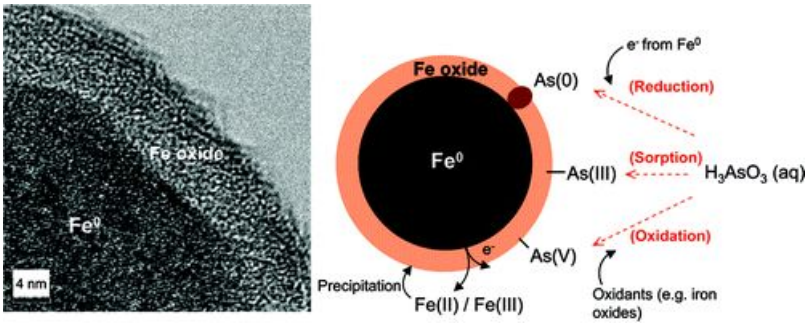

FIGURE 2.2: Schematic diagram of nZVI core-shell structure
Source: [32].

In summary, nZVI are reactive iron nanoparticles used for remediation. The particles corrode, aggregate, and settle in groundwater because of the high particle-particle and particle-collector electrostatic, magnetic and van der Waals interactions.

Chapter 3

Aggregation of nZVI

The aggregation of particles is caused by many processes that generally occur during particle migration. The decrease in mobility can be formulated by a rate of aggregation given by the mass transport coefficients (MTC) β [m^3/s]. These coefficients represent a frequency of collisions between particles. Due to the attractive Van der Waals forces, collisions lead to aggregation of the particles (the particles remain adherent). Models of aggregation of small particles have been published in many articles (e.g. [3, 10, 33]). These are mostly based on the publications [1], [2](GL).

The coefficients give a probability P_{ij} of the creation of an aggregate from particle i and particle j together with numbers n_i, n_j of particles i and particles j in one m^3 (3.1). n_i can be also called particle concentration in this work. The probability means a frequency of collision between i and j particles. Particle i means the aggregate created from i elementary nanoparticles. It was published in [3].

$$P_{ij} = \beta_{ij}\, n_i\, n_j, \tag{3.1}$$

$$\beta_{ij} = \beta_{ij}^1 + \beta_{ij}^2 + \beta_{ij}^3. \tag{3.2}$$

Coefficient β_{ij}^1 is the mass transport coefficient of heat fluctuation, coefficient β_{ij}^2 is the mass transport coefficient for velocity gradients, and the coefficient β_{ij}^3 is the mass transport coefficient of aggregation caused by gravity. The concept is adopted from [3]. A detailed derivation summary of the MTC was presented in author's diploma thesis [9].

$$\beta_{ij}^1 = \frac{2\, k_B\, T}{3\, \eta}\, \frac{(d_i + d_j)^2}{d_i\, d_j}, \tag{3.3}$$

where k_b is the Boltzman constant, T is the absolute temperature, η is the viscosity of the medium and d_i is the diameter of the particle i.

$$\beta_{ij}^2 = \frac{1}{6}\, G\, (d_i + d_j)^3, \tag{3.4}$$

where G is $\frac{\partial v}{\partial n}$ representing velocity gradient of the liquid.

$$\beta_{ij}^3 = \frac{\pi\, g}{72\, \eta}\, (\varrho_p - \varrho)\, (d_i + d_j)^2\, |d_i^2 - d_j^2|, \tag{3.5}$$

where g is the gravity acceleration, η is the viscosity of the medium, ϱ is the density of the medium, and ϱ_p is the density of the aggregating particles.

Chapter 4

Inclusion of Electrostatic forces into MTC

Particles in an electrolyte have a surface charge density σ with dimension [C/m^2], depending on the pH and ionic strength of water. The magnitude of the surface charge density gives a long-range repulsive electrostatic force between particles. We added the force into the mass transport coefficients for all three processes (β^1 (3.3), β^2 (3.4), and β^3 (3.5)). The electrostatic force F_c is given by Coulomb's law

$$F_c = \frac{1}{4\pi\varepsilon_0\varepsilon}\frac{Q_i Q_j}{R^2} \tag{4.1}$$

where ε is the dielectric constant of the liquid, ε_0 is the vacuum permittivity, R is the distance between the centres of gravity of the particles i and j, Q_i is the charge of the particle i [C]. Particle charge $Q_i = \sigma_i S_i$, where S_i is the surface of particle i.

$$Q_i = \sigma_i \pi d_i^2;$$

$$F_c = \frac{\pi}{4\pi\varepsilon_0\varepsilon}\frac{\sigma_i\sigma_j d_i^2 d_j^2}{R^2}. \tag{4.2}$$

The mass transport coefficient with electrostatic forces for Brownian diffusion can be presented as follows

$$\beta_{ij}^{1,el} = \frac{2\,k_B\,T}{3\,\eta}\,\frac{(d_i+d_j)^2}{d_i\,d_j} - \frac{\pi\,d_i^2\,d_j^2\,\sigma_i\sigma_j}{3\,\eta\,\varepsilon_0\,(d_i+d_j)}, \tag{4.3}$$

where σ_i and σ_j stand for surface charge on particle i and particle j, respectively. If a component that reduces the mass transport coefficient is bigger than the mass transport coefficient without the influence of electrostatic forces, the probability of collision of particles i and j will be equal to zero. That is why we set

$$\tilde{\beta}_{ij}^{1,el} = \max(0, \beta_{ij}^{1,el}). \tag{4.4}$$

The mass transport coefficient for the velocity gradients $G = \frac{\partial v}{\partial n}$ including the effect of electrostatic forces has the form

$$\beta_{ij}^{2,el} = \frac{1}{6} G \left(d_i + d_j\right)^3 - \frac{\pi \, d_i^2 \, d_j^2 \, \sigma_i \sigma_j}{12 \, \eta \, \varepsilon_0} \left| \frac{1}{d_i} + \frac{1}{d_j} \right|. \tag{4.5}$$

$$\tilde{\beta}_{ij}^{2,el} = \max(0, \beta_{ij}^{2,el}). \tag{4.6}$$

The mass transport coefficient including the impact of electrostatic forces for the sedimentation is

$$\beta_{ij}^{3,el} = \frac{\pi \, g}{72 \, \eta} \left(\varrho_p - \varrho\right) \left(d_i + d_j\right)^2 \left| d_i^2 - d_j^2 \right| - \frac{\pi \, d_i^2 \, d_j^2 \, \sigma_i \sigma_j}{12 \, \eta \, \varepsilon_0} \left| \frac{1}{d_i} - \frac{1}{d_j} \right|, \tag{4.7}$$

$$\tilde{\beta}_{ij}^{3,el} = \max(0, \beta_{ij}^{3,el}). \tag{4.8}$$

The probability of coagulation decreases quadratically with the increasing charge. The probability of collision between particles i and j is determined by the density of these particles and by the sum of the mass transport coefficients

$$P_{ij}^{el} = \left(\tilde{\beta}_{ij}^{1,el} + \tilde{\beta}_{ij}^{2,el} + \tilde{\beta}_{ij}^{3,el} \right) n_i \, n_j. \tag{4.9}$$

Chapter 5

Sectional aggregation model

Gen-tran is the software used at the Technical University of Liberec to compute reactions between entities in water. Here, it was required to compute reactions between the aggregates (particles), describing collisions of two aggregates leading to the creation of one aggregate. There are over a million of aggregates with different sizes and different transport properties in a dispersion of unstable particles. It is not possible to compute reactions between the millions of entities, therefore it was necessary to generate a system for clustering particles into several categories, which are here called "sections", according to their size. Particles with similar size have similar transport properties. We can observe migration of the particle size sections (PSS) instead of observing every single aggregate. Thereafter, we can estimate a distribution of the sections in the media and their percentage giving a good insight into how the dispersion would migrate in the medium.

We based the clustering model on the sectional representations for simulating aerosol dynamics published in the paper [16]. This chapter describes the sectional model.

With this model, it is possible to compute a change in particle number, volume and surface area, and to estimate a rate of aggregation over time. An example is given in Fig. 5.1, where a change in the number of particles in sections is expressed. The number of particles is expressed as a percentage ratio of the starting value. The results were computed using Matlab R2009a. The values of number changes were computed for three sections including particles with radii according to the label in Fig. 5.1. The starting value of particle number was $2.17 \cdot 10^{17}$ nanoparticles in 1 L, radius of one nanoparticle is 20 nm, surface charge density is $2.5 \cdot 10^{-5}$ Cm^{-2}, density of particles is 6700 $\mathrm{kg/m}^3$, temperature is 300 K, dynamic viscosity of water is 10^{-3} Pa·s, density of water is 1000 $\mathrm{kg/m}^3$, velocity gradient is 50 s^{-1}.

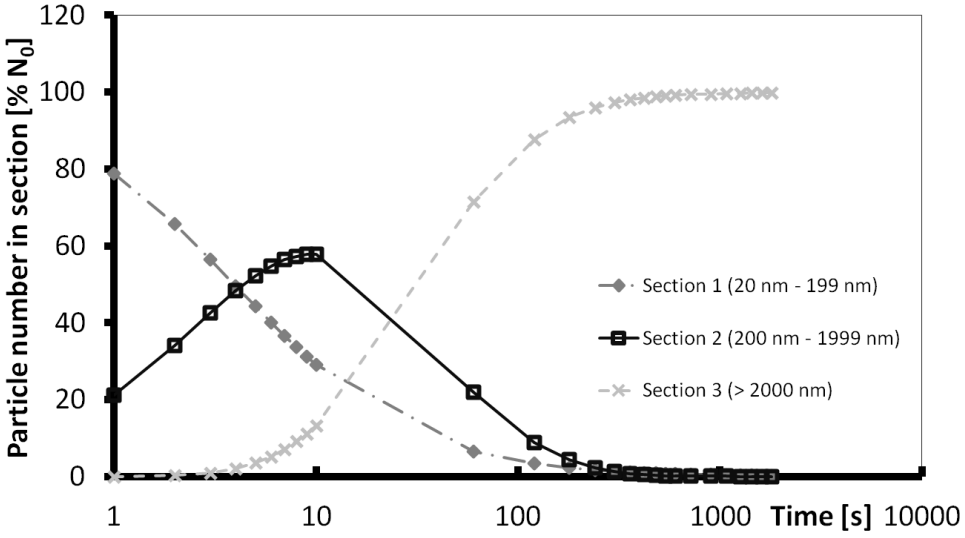

FIGURE 5.1: Computed change of number of particles caused by the aggregation in 30 time steps

Chapter 6

Magnetic nanoparticle aggregation

nZVI exposed to water acquires an oxide shell. For example, RNIP particles manufactured by Toda Kyogo, Japan, have a Fe^0 core and a magnetite (Fe_3O_4) shell [6, 28]. Both Fe^0 and Fe_3O_4 are magnetic so magnetic attractive forces between particles may also affect the dispersion stability [34]. The influence of the magnetic properties of iron nanoparticles on their aggregation is apparent under an applied magnetic field, where ferromagnetic or paramagnetic dispersions form chain-like aggregates in which the dipoles are oriented in a head-tail configuration along the direction of the field [14]. Hence, an nZVI dispersion might undergo dipole-dipole attraction between the magnetic moments of the particles which may affect their size and dispersion stability.

According to [35], the electromagnetic potential at the point $\vec{r}$ near a permanent magnet is equal to

$$\phi(\vec{r}) = \int_V \frac{\vec{M}\vec{R}}{R^3} dV, \tag{6.1}$$

where the vector $\vec{M}$ is the vector of magnetization at the point dV, the vector $\vec{R}$ is the difference between the source of the magnetic field dV and the point $\vec{r}$, R is the length of $\vec{R}$.

The intensity of the magnetic field $\vec{H}$ can be subsequently computed as

$$\vec{H}(\vec{r}) = -g\vec{r}ad(\phi(\vec{r})). \tag{6.2}$$

Finally, the magnetic force between the source of the intensity of the magnetic field $\vec{H}$ and a permanent magnet with the magnetization $\vec{M}_0$ at the point $\vec{r}$ is equal to

$$\vec{F}(\vec{r}) = -\int_V (\vec{M}_0 \cdot g\vec{r}ad)\vec{H}(\vec{r}) dV. \tag{6.3}$$

The scalar potential of the magnetic field around one homogeneous spherical iron nanoparticle with radius a located at the point $[0, 0, 0]$ was determined to be:

$$\phi(\vec{r}) = M \int_0^{2\pi} \int_0^{\pi} \int_0^{a} \frac{(x_3 - r' \cos(\theta)) r'^2 \sin(\theta)}{\sqrt[3]{(x_1^2 + x_2^2 + x_3^2 - r'^2)^2}} dr' d\theta d\varphi, \tag{6.4}$$

where a is the radius of the nanoparticle and $[x_1, x_2, x_3]$ are the coordinates of the point $\vec{r}$. The direction of the magnetization vector $\vec{M}$ is set to the direction x_3 and M is the magnitude of the vector $\vec{M}$.

An aggregate of iron nanoparticles is in fact a clump of many permanent magnets. The statistical model of aggregation assumes that the volume of the aggregate is filled by uniformly distributed nanoparticles (small homogeneous magnets) with randomly uniformly distributed direction of magnetization (an assessment of the real structures of an aggregate is in thesis in Chapter 7). The magnitude of the magnetization vector of all nanoparticles is the same. The magnetic potential of the aggregate is then the sum of the magnetic potentials of all nanoparticles creating the aggregate:

$$\phi(\vec{r}) = \sum_{i=1}^{N_p} \phi_i(\vec{r} - \vec{r}_i), \tag{6.5}$$

where ϕ_i is the potential of the magnetic field of the nanoparticle i located at the point $\vec{r}_i$, N_p is the number of nanoparticles in the aggregate.

The magnetic force between two aggregates is the sum of magnetic forces between all pairs of nanoparticles from the two aggregates (between every nanoparticle from the first aggregate and every nanoparticle from the second aggregate):

$$\vec{F}_A(\vec{r}) = \sum_{i=1}^{N_{p,1}} \sum_{j=1}^{N_{p,2}} \vec{F}_{ij}, \tag{6.6}$$

where $\vec{F}_A$ is the magnetic force between two aggregates, $\vec{F}_{ij}$ is the magnetic force between i-th nanoparticle in the first aggregate and j-th nanoparticle in the second aggregate, $N_{p,1}$, $N_{p,2}$ is the number of nanoparticles in the first and second aggregate respectively.

The effect of magnetic forces was assessed using the value “limit distance”. Up to this distance from the centre of an aggregate, the attractive magnetic forces cause the aggregation of the aggregate and a particle placed inside this range. In ranges larger than the limit distance, other forces outweigh the magnetic forces. The limit distance value gives the loci in which the gravitational and magnetic forces affecting the aggregate are equal (6.7).

$$F_g = F_{mg}(L_d), \tag{6.7}$$

where $F_{mg}(L_d)$ is the magnetic force computed at the distance L_d from the centre of the observed particle.

The limit distance is estimated using (6.8) as a starting distance for the next iteration.

$$L_{d,0} = \sqrt[4]{\frac{F_{mg}(R_0)}{F_g}} R_0. \tag{6.8}$$

The next computation of $L_{d,s+1}$ applies to particles placed at distance $L_{d,s}$ and uses the magnetic force computed with the corrected value of the distance $F_{mg}(L_{d,s})$, where $s = 0, \ldots s_{max}$ is the number of iteration, s_{max} is chosen maximum number of iterations or the last iteration step when a chosen condition is satisfied.

$$L_{d,s+1} = \sqrt[4]{\frac{F_{mg}(L_{d,s})}{F_g}} L_{d,s}. \tag{6.9}$$

Chapter 7

Structure of Aggregates

The structure that nanoparticles form in the aggregate is not known - that is, the position of the nanoparticles in the aggregate and the direction of their magnetization vector. This knowledge is crucial in order to compute the magnetic forces between aggregates. In this chapter, various aggregate structures are examined and assessed.

An unstructured model of an aggregate $A(n, \vec{R})$ composed of n nanoparticles with its centre at position $\vec{R}$ is a set of n nanoparticles so that all of the nanoparticles are spheres of constant radius a and constant saturation magnetization M and their centres $\vec{r_i}$ $(i \in \{1, \ldots, n\})$ are uniformly randomly distributed inside the sphere with centre at $\vec{R}$ and radius $\sqrt[3]{n}a$, and the directions of the saturation magnetization vectors $\vec{M_i}$ are uniformly randomly (Fig. 7.1) or equally (Fig. 7.2) distributed in the individual sphere.

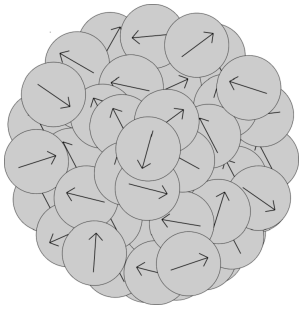

FIGURE 7.1: An unstructured model of an aggregate with randomly directed vectors of magnetization of nanoparticles creating the aggregate

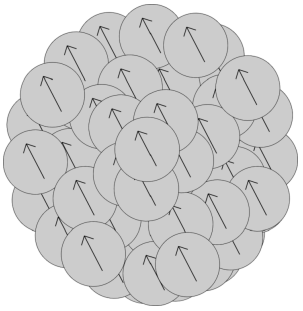

FIGURE 7.2: An unstructured model of an aggregate with the same direction of vectors of magnetization of nanoparticles creating the aggregate

As it was expected, when nanoparticles have the same direction of magnetization, the attractive magnetic force of the aggregate created by the nanoparticles have a longer range than when the nanoparticles have randomly directed magnetization. A significant attribute of the unstructured model of the aggregate is the size of the magnetic force in comparison with the size of the other forces affecting the aggregate movement. The

computed magnetic forces are bigger than the counteracting gravitational force and the aggregation rate increases.

The alternative aggregate structure is that the nanoparticles arrange themselves in a structured order in the aggregate. Vectors of magnetization of the nanoparticles adhere to the structure. According to the observed behaviour of spherical magnets, the magnets create sections with the minimum of energy. With a small number of magnets, most sections are created in circles composed of chains. Other structured models of aggregates were also considered - namely, cubic and honeycomb. The directions of vectors of magnetization of nanoparticles in these models of structured aggregates are shown in Fig. 7.3.

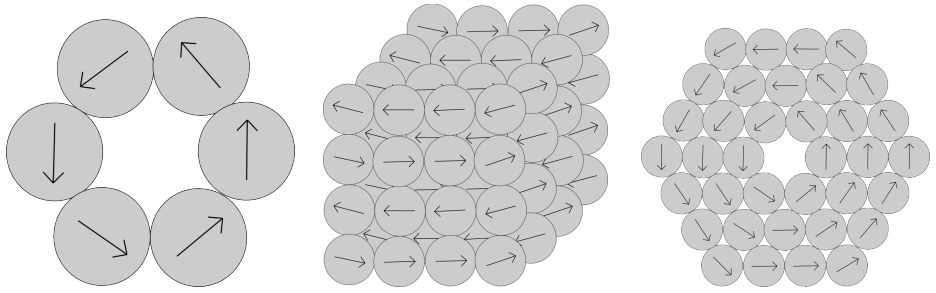

(a) Circle structure (b) Cube structure (c) Hexagon structure

FIGURE 7.3: Diagram of the structure of nanoparticles creating an aggregate with schematic directions of magnetization vectors of the nanoparticles

For structured aggregates with magnetization of nanoparticles adhering to the structure, the magnetic forces have an insignificant influence on the rate of aggregation of the particles. That does not match the observations [14]. Therefore, on the basis of the results in this section, it was decided not to study more structured forms. The structure of real aggregates was assumed to be damaged.

Another way to assess the most probable structures of aggregates is by computing the interaction energy E between nanoparticles which make up the aggregate. According to [36]:

$$E = -\vec{m} \cdot \vec{B}. \tag{7.1}$$

E is the potential energy that a magnetic moment $\vec{m}$ has in an externally-produced magnetic field $\vec{B}$.

According to the results in the thesis, the most probable structure for small aggregates is chains and for bigger aggregates is spherical sections with the same direction of magnetization vectors of nanoparticles creating the aggregate.

Chapter 8

Methods of computing magnetic forces

The magnetic forces interacting between two aggregates can be computed in two ways. The more correct one called summation and the more rapid one called averaging.

The *method of summation* is based on the accurate computation by the summation of magnetic forces between every nanoparticle in the first aggregate and every nanoparticle in the second aggregate: The magnetic field around the first aggregate $A(n_1, \vec{0})$ is computed as the sum of the magnetic fields of every single nanoparticle creating the aggregate:

$$\tilde{\phi}(\vec{r}) = \sum_{i=1}^{n_1} \phi(\vec{r} - \vec{r}_{1i}, \vec{M}_{1i}, a), \tag{8.1}$$

where ϕ is computed using the formula (6.4) rotated to the direction of magnetization M_{1i}, $\vec{r}_{1i}$ is the location of the centre of the i-th nanoparticle in the first aggregate, and $\vec{M}_{1i}$ is the magnetization vector of the i-th nanoparticle in the first aggregate.

The magnetic force acting on the second aggregate $A(n_2, \vec{R})$ is then computed as the sum of the magnetic forces acting on every single nanoparticle in the second aggregate:

$$\vec{F} = \sum_{j=1}^{n_2} \tilde{V}(\vec{M}_{2j} \cdot \vec{grad}) \vec{grad} \tilde{\phi}(\vec{r}_{2j}) \tag{8.2}$$

where $\tilde{V} = \frac{4}{3}\pi a^3$ is the volume of a nanoparticle, $\vec{r}_{2j}$ is the location of the centre of the j-th nanoparticle in the second aggregate and $\vec{M}_{2j}$ is the magnetization vector of the j-th nanoparticle in the second aggregate.

The *method of averaging* works with aggregates with averaged magnetization vector according to the following formula:

$$\vec{M}_A = \frac{\sum_{i=1}^{n} \vec{M}_i}{n}. \tag{8.3}$$

where $\vec{M}_A$ is the averaged magnetization vector of the aggregate A and $\vec{M}_i$ is the vector of magnetization of the i-th nanoparticle from the aggregate A. The magnetic force between $A(n_1, \vec{0})$ and $A(n_2, \vec{R})$ is approximated by the formula

$$\vec{F} \doteq V_2(\vec{M}_{2A} \cdot g\vec{r}ad)g\vec{r}ad\phi(\vec{R}, \vec{M}_{1A}, \sqrt[3]{n_1}a) \tag{8.4}$$

where $\vec{M}_{1A}$ and $\vec{M}_{2A}$ are the averaged magnetization vectors of the aggregates $A(n_1, \vec{0})$ and $A(n_2, \vec{R})$ respectively, $V_2 = \sqrt[3]{n_2}a$ is the volume of the second aggregate and $\phi(\vec{R}, \vec{M}, V)$ is the electromagnetic potential of the averaged aggregate computed analogously to (6.1):

$$\phi(\vec{R}, \vec{M}, V) = \int_V \frac{\vec{M}\vec{R}}{R^3} dV. \tag{8.5}$$

Chapter 9

Inclusion of electrostatic forces in the computation of the limit distance

Due to long-range attractive magnetic forces, forces acting on the particles not only in close proximity R_0 but also in further distances are of interest. The question is how large the repulsive electrostatic force is at the limit distance L_d and how it affects the attraction of particles.

The magnitude of the electrostatic force is a function of the distance between particles as well as the strength of the magnetic force. Therefore, we decided to include computation of the effect of the electrostatic force once more directly into the limit distance computation. There is another way to compute the effect of electrostatic forces between particles but more suitable for the case of particles upon which the long-range forces act.

The extension was achieved by adding Coulomb's law F_c (4.2) into the equilibrium equation of the forces acting on the aggregating particle. In this case, the equation was expressed in terms of attractive magnetic force on one side and counteracting gravitational force on the other (6.7). By including the repulsive electrostatic force, the limit distance that expresses the border of particle mutual attraction leading to aggregation of particles is reduced depending on the surface charge density of the particles.

Because the magnetic force decreases to the power 4 and Coulomb's force to the power 2, the equilibrium equation of forces takes the form:

$$F_g + F_c \frac{R_0^2}{L_d^2} - F_{mg} \frac{R_0^4}{L_d^4} = 0. \tag{9.1}$$

The limit distance estimated by (9.2) is used as a starting distance for the next iteration.

$$L_{d,0}^{el} = \sqrt{\frac{\sqrt{F_c^2(R_0) + 4F_g F_{mg}(R_0)} - F_c(R_0)}{2F_g}} R_0. \tag{9.2}$$

The next computation of $L_{d,s+1}^{el}$ is performed with particles placed at distance $L_{d,s}^{el}$ and using the magnetic force and electrostatic force computed with the corrected value of distance $F_{mg}(L_{d,s}^{el})$ and $F_c(L_{d,s}^{el})$ respectively.

$$s = 0, \ldots s_{max},$$

where s is the number of iteration, s_{max} is chosen maximum number of iterations or the last iteration step when a chosen condition is satisfied.

$$L_{d,s+1}^{el} = \sqrt{\frac{\sqrt{F_c^2(L_{d,s}^{el}) + 4F_g F_{mg}(L_{d,s}^{el})} - F_c(L_{d,s}^{el})}{2F_g}} L_{d,s}^{el}. \tag{9.3}$$

A comparison between the computation of the limit distance with and without electrostatic forces is in Fig. 9.1, 9.2. The limit distance was computed with the values: diameter of one nanoparticle is 50 nm, size of magnetization vector is 570 kA/m, surface charge of all particles is either 10^{-6} or $2.5 \cdot 10^{-5}$ C/m^2 (these values were chosen on the basis of the values ascertained for low and high effect of electrostatic forces between particles on the aggregation rate). The unstructured model of aggregates with the same direction of magnetization was used for the computation. The computed limit distances are shown in Fig. 9.1 and 9.2. The values of limit distances computed using equation (9.2) are compared with values of the limit distance computed by the equation excluding the effect of the electrostatic forces (6.8).

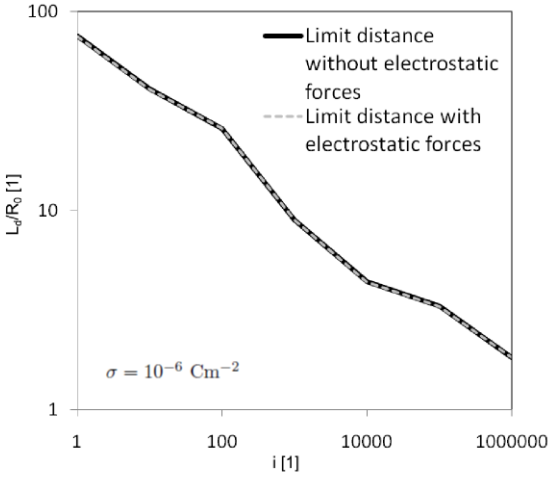

FIGURE 9.1: Limit distance values with and without electrostatic force inclusion
The surface charge of particles is 10^{-6} C/m^2

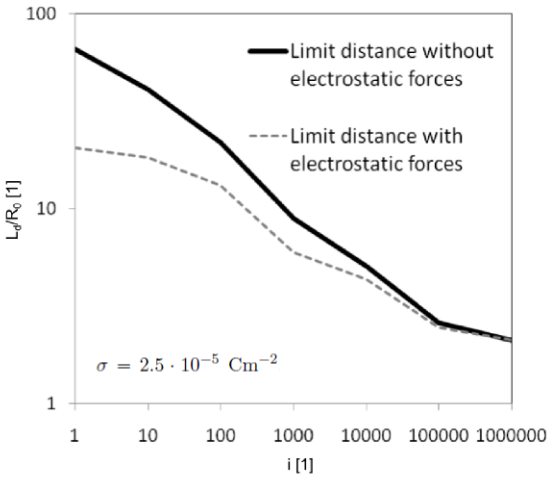

FIGURE 9.2: A comparison of limit distances with and without consideration of the effect of electrostatic forces with surface charge of particles $2.5 \cdot 10^{-5}$ C/m^2

In the graphs, the limit distance is not expressed in absolute values but as the ratio of the limit distance and the distance between the centres of the interacting particles attached to each other $\frac{L_d}{R_0}$. This represents how many times the distance between the centres of particles had to be increased in order not to aggregate due to magnetic forces. The comparison was performed for one nanoparticle interacting with aggregates of different sizes comprised of i nanoparticles.

It can be seen that in the case of higher ζ potential, the limit distance of magnetic forces is decreased. Hence it is important to include the effect of electrostatic forces as well as the effect of magnetic forces in the determination of the aggregation rate of particles.

Chapter 10

MTC extended by electrostatic and magnetic forces

If the particles are magnetic but have zero surface charge density, the mass transport coefficient (MTC) of particles i and j is equal to

$$\beta_{ij}^{mg} = \beta_{ij}^{1,mg} + \beta_{ij}^{2,mg} + \beta_{ij}^{3,mg}. \tag{10.1}$$

$$\beta_{ij}^{1,mg} = \frac{4\,k_B\,T}{3\,\eta}\,\left(\frac{1}{d_i} + \frac{1}{d_j}\right)\,L_d, \tag{10.2}$$

$$\beta_{ij}^{2,mg} = \frac{4}{3}\,G \cdot L_d^3, \tag{10.3}$$

$$\beta_{ij}^{3,mg} = \frac{\pi\,g}{18\,\eta}\,(\varrho_p - \varrho)\,|d_i^2 - d_j^2|\,L_d^2. \tag{10.4}$$

If the particles have non-zero surface charge density and magnetization, the mass transport coefficient (MTC) of particles i and j is equal to

$$\beta_{ij}^{mg,el} = \beta_{ij}^{1,mg,el} + \beta_{ij}^{2,mg,el} + \beta_{ij}^{3,mg,el}. \tag{10.5}$$

$$\beta_{ij}^{1,mg,el} = \frac{4\,k_B\,T}{3\,\eta}\,\left(\frac{1}{d_i} + \frac{1}{d_j}\right)\,L_d^{el}, \tag{10.6}$$

$$\beta_{ij}^{2,mg,el} = \frac{4}{3}\,G \cdot \left(L_d^{el}\right)^3, \tag{10.7}$$

$$\beta_{ij}^{3,mg,el} = \frac{\pi\,g}{18\,\eta}\,(\varrho_p - \varrho)\,|d_i^2 - d_j^2|\,\left(L_d^{el}\right)^2. \tag{10.8}$$

The comparison was performed for an extreme case with a spherical aggregate structure with the same direction of magnetization vectors of all nanoparticles creating the aggregates. This model of aggregate structure shows the highest possible aggregation rate. The mass transport coefficients β_{ij} computed by the model of particle aggregation

at a distance of R_0 (3.2) apart are compared with the mass transport coefficients of particles at distance L_d including magnetic forces β_{ij}^{mg} (10.1) and also with the mass transport coefficients computed at distance L_d^{el} including both magnetic forces and electrostatic forces $\beta_{ij}^{mg,el}$ (10.5). Computation of L_d and L_d^{el} for the magnetic forces was performed using the method of averaging for particles with ratio L_d/R_0 higher than 15, otherwise it was performed accurately using the method of summation.

The MTC values in Fig. 10 were computed using the following values: diameter of one nanoparticle is 50 nm, density of particles is 6700 kg/m^3, temperature is 300 K, dynamic viscosity of water is 10^{-3} Pa·s, density of water is 1000 kg/m^3, velocity gradient is 50 s^{-1}, size of magnetization vector is 570 kA/m and the surface charge of all particles is 10^{-6} Cm^{-2}.

The results of the size of the effect of magnetic forces were summarized and included into an analytical model of collisions between magnetic nanoparticles. Due to attractive magnetic forces, the aggregation rate is significantly higher and the repulsive electrostatic forces are almost negligible (Fig. 10). It is assumed that with other realistic choices of values of magnetization vector or surface charge, this trend would not change dramatically.

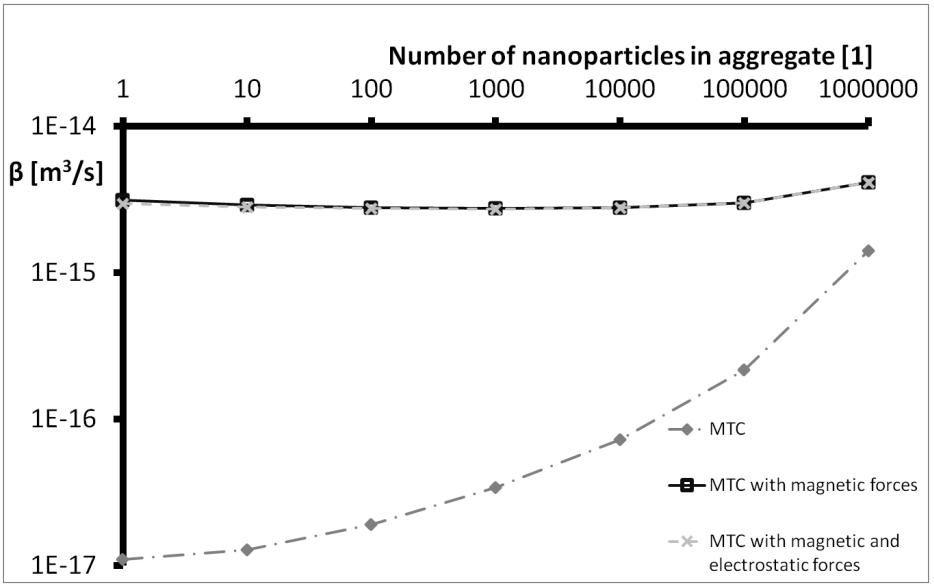

FIGURE 10.1: A comparison of MTC computed with and without the effect of electrostatic and magnetic forces

This modified model of aggregation better explains the rapid aggregation of zero-valent iron nanoparticles that is observed. This can help to simulate the migration of undissolved particles in groundwater.

Chapter 11

Adaptation of aggregation model to kinetic reactions

In chapter 5, the aggregation between particles was transformed to a model of aggregation between particle size sections (PSS) described by mass transport coefficient (MTC) giving the frequency of aggregation between particles from different sections.

The dynamics of aggregation correspond to a first-order reaction Re where two particles from different or the same sections aggregate (react) and a single particle is formed. Velocity of reactions is given by rate of change v_R which is proportional to rate constant k_R and concentrations of reacting species (concentrations c_r and c_p of aggregates from sections r and p respectively):

$$v_R = k_R c_p c_r.$$

The change in concentration of the particles in observed section l over time t is:

$$\frac{dc_l}{dt} = S_R(l) \cdot v_R = S_R(l) k_R c_p c_r, \tag{11.1}$$

where S_R is the stoichiometry [1]. Here, the rate constant k_R has the unit [l/g/s].

Under the assumption of constant number of nanoparticles, the total volume of all particles in one section is equal to the total number of nanoparticles forming all the particles in the section multiplicated by the volume of a single nanoparticle. The change of total volume of a section can be evaluated as the change of number of all nanoparticles forming particles in the observed section. The change is given by aggregation of particles from smaller sections forming particles from larger sections. Because the change of volume of all nanoparticles in each section is being observed, reactions inside one section (both aggregating particles and also the resulting one belong into the same section) are not of interest.

The aggregation rate can be given by MTC $\hat{\beta}^{+}_{r,p,l}$ which is the mass transport coefficient of an increase of particles in the observed section l formed by the aggregation of the particles from sections r and p. A change in the particle concentration n_l in the section l follows:

$$\frac{dn_l}{dt} = \hat{\beta}^{+}_{r,p,l} n_p n_r. \tag{11.2}$$

The rate constant k_R can be calculated from the MTC $\hat{\beta}^{+}_{r,p,l}$.

$$k_R = \frac{1}{S_R(l)} \hat{\beta}^{+}_{r,p,l} \frac{1}{m_0} \frac{A_l}{A_r A_p}. \tag{11.3}$$

The weight of a single nanoparticle is m_0. The value of A_l is not set by any theory, so the following choice of average aggregate size was chosen: $A_l = \frac{k_l - k_{l-1}}{2}$ where k_l is the number of the nanoparticles which make up the largest possible aggregate belonging in section l (see chapter 5). The stoichiometry S_R has been also derived from the volume of the aggregates (number of the nanoparticles) in aggregating sections. By convention, the stoichiometries for reactants are negative and for products positive.

Chapter 12

Simulation of transport of aggregating nanoparticles

In this chapter in thesis, simulations of nanoparticle transport and aggregation to verify the theoretical aggregation models are provided. Firstly, an experiment of bentonite colloidal particles through a granite was simulated. The particles had non-zero surface charge but were not magnetic. Therefore, the simulation of particle aggregation was computed using the model from Chapter 4. The model describes an aggregation of nanoparticles caused by their oscillation, different velocities during sedimentation and drifting in water, and mutual repulsion due to electrostatic forces. Secondly, a simulation of experiments of one-dimensional nZVI particle migration was done. This simulation served to verify an aggregation model with inclusion of both magnetic and electrostatic forces. The transformation of mass transport coefficients into kinetics was tested on this simulation. Thirdly, we tested out a possibility of simulation of a real nZVI migration in ground when the nanoparticles were used for remediation of a real area. Despite the fact that measurements on the chosen location were well documented and quite frequent, results of the measurements of nanoparticle concentration were too sparse to do a good simulation.

Benefits of transport model including particle aggregation effect on transport are in improvement of theoretical understanding of transport of unstable nanoparticles. This improvement could be useful for softwares simulating transport of aggregating particles, however, in good documented problems. It can be useful also in situation when an aggregation of particles is crucial - for example for computation of age of nanoparticles before their usage (how aggregated they are).

Chapter 13

Conclusions

Zero-valent iron nanoparticles are increasingly being used for water and soil treatment as a highly reactive, easily transportable, nontoxic remedial agent. However, it was found that the nanoparticles aggregate so rapidly that they quickly lose their high reactivity and transportability, which are the crucial parameters. This is caused mostly by the long-range attractive magnetic forces acting between the nanoparticles. The thesis has developed a theoretical model of aggregation of the migrating nanoparticles that includes the effect of repulsive electrostatic and the attractive magnetic forces acting between the particles. The model has then been modified for practical usage and is a proven improvement compared to the basic model of aggregation.

The benefits of the improved aggregation model are evident in the better theoretical understanding of the interactions between nanoparticles. The system of aggregation rate computation developed in this thesis can be used for the computation of the age of nanoparticles before their use which could lead to better utilization of the material and cost-saving. The transport model including the effect of particle aggregation on transport can be included into software which simulates the transport of aggregating particles, both for scientific and practical purposes. This concluding chapter summarizes the work presented in the thesis and suggests some future directions.

13.1 Summary of work

The aim of the thesis has been to research the interactions between magnetic nanoparticles with non-zero surface charge that are transported through a porous medium. We started with an aggregation model described by mass transport coefficients between particles computed on the basis of the heat fluctuation of particles and their different velocities during sedimentation and drifting in water. The coefficients gave a frequency of collisions between particles. The derivation of the coefficients is summarized in Chapter 3.

Particles with high surface charge values repel each other and the rate of aggregation falls. We included the effect of electrostatic forces into the aggregation model in Chapter 4. In order to verify the new models, we modified a sectional model of aggregation, which allowed the computation of the reactions between particle size sections. Particles were divided into sections according to their size. Aggregation of particles does not have to be computed between each individual aggregate that occurs in the particle dispersion. The whole derivation of sectional model and modification of the mass transport coefficients for the model is detailed in Chapter 5.

The effect of magnetic forces on the aggregation rate was assessed in the Chapter 6. The magnitude of the magnetic force between two nanoparticles was derived as well as the magnetic field around an aggregate. The impact of the magnetic force on the aggregation rate was determined by using the value of the limit distance that gives the minimal distance between particles needed for particles not to aggregate due to their attractive magnetic forces.

In Chapter 7, the influence of the structure of nanoparticles in aggregates on the resulting magnetic field around the aggregates was examined. The parameters to be compare were the magnitude of the magnetic forces between particles and the limit distance. According to these two connected parameters, it was possible to estimate the degree of influence of the magnetic forces on the aggregation rate of particles. Then, the probable aggregate structure was examined on the basis of the interaction energy between the nanoparticles in an aggregate.

Since the computation of the magnetic forces is time consuming, two methods of estimating the magnetic forces are presented here – the simple and fast averaging of averaging and the more precise, but more time consuming summation method are discussed in Chapter 8. It was found that the best way to generalize the results is to relate the distance between two particles to the shortest possible distance R_0, which is the sum of radii of the investigated pair of aggregates. The limit where the averaging method could be used is the distance over $10 \cdot R_0$ between particles. When the particles are closer to each other than $10 \cdot R_0$, the magnetic forces between the particles must be estimated using the slow, but more complex summation method. Otherwise, the averaging method can be used for computation.

Another way of including electrostatic forces into the aggregation model is examined in Chapter 9. The repulsive electrostatic forces are long-range as well as the attractive magnetic forces, therefore we added the electrostatic force effect directly in the limit distance model. In Chapter 10, the limit distance was used as an area around an aggregate in which the flux of other particles is observed. The mass transport coefficients are computed on the basis of this limit distance value that increases the aggregation rate. The model of aggregation computation was transferred to kinetics in Chapter 11. The aggregation between sections is calculated in the form of kinetic equations, which is

useful for computing the transport of entities and the reactions between them in various software.

The aggregation model, with includes both electrostatic and magnetic forces was tested on simulations of particle transport in Chapter 12. First, the transport of non-magnetic particles with surface charge was simulated using the aggregation model from Chapter 4. Then, a one-dimensional model of the transport of magnetic nanoparticles with surface charge was simulated and the aggregation model from Chapter 10 was tested together with the transformation of mass transport coefficient into kinetics from Chapter 11. In the last section, the suitability of the aggregation model which includes electrostatic and magnetic forces was examined for the simulation of a real iron nanoparticle injection into ground.

13.2 Future work

A large part of the thesis has been concerned with the description of magnetic forces between iron nanoparticles and their inclusion in the aggregation model used for simulating the transport of aggregating particles. Whilst some progress has been made in describing aggregating particle transport, there is much scope for further investigation. In this section, some suggestions of possible themes for additional investigations are discussed.

In Chapter 7, the possible structure of aggregates that are important for the magnetic force of aggregates computation were examined. It was found out that firstly, a small chain of magnetic nanoparticles, then sections of nanoparticles are formed. At some point, the aggregated sections stop creating larger sections and they only attach to another chain of sections. This process should be taken into account. Our computations only account for spherical aggregates.

In Chapter 6, the limit distance is computed from the equilibrium equation of forces in which the only counteracting force against the magnetic force is gravity. For a more accurate description of the effect of magnetic forces, the others forces acting on the aggregating particles should be included in the equilibrium of forces and the limit distance computation.

Another simplification that was used was the presumption that the surface charge of all aggregates is constant and uniformly distributed on the surface of the aggregates. An investigation into the reality of the situation and its inclusion in the aggregation model could be another additional investigation. It is connected to the ageing of iron nanoparticles in a dispersion where the surface of the particle corrodes, changes and so do the properties of the particles, such as the surface charge, magnetization, etc.

When we investigate the transport of reactive unstable particles, attachment of the particle to the pore surface should also be taken into account as a factor that slows down particle transport and prevents particle migration through the ground.

Bibliography

[1] Camp TR, Stein PC: *Velocity Gradients in Internal Work in Fluid Motion*. MIT 1943.

[2] Smoluchowski M: **Versuch einer mathematischen Theorie der Koagulationskinetik kolloider Lösungen**. *Z. Phys. Chem.* 1917, **92**:129–168.

[3] Buffle J, Leeuwen HPv: *Environmental Particles*. CRC Press, 1 edition 1992.

[4] Zhang Wx: **Nanoscale Iron Particles for Environmental Remediation: An Overview**. *Journal of Nanoparticle Research* 2003, **5**(3):323–332.

[5] Li L, Fan M, Brown RC, Van Leeuwen JH, Wang J, Wang W, Song Y, Zhang P: **Synthesis, Properties, and Environmental Applications of Nanoscale Iron-Based Materials: A Review**. *Critical Reviews in Environmental Science and Technology* 2006, **36**(5):405–431.

[6] Nurmi JT, Tratnyek PG, Sarathy V, Baer DR, Amonette JE, Pecher K, Wang C, Linehan JC, Matson DW, Penn RL, Driessen MD: **Characterization and properties of metallic iron nanoparticles: spectroscopy, electrochemistry, and kinetics**. *Environmental Science & Technology* 2005, **39**(5):1221–1230.

[7] Filip J, Zboril R, Schneeweiss O, Zeman J, Cernik M, Kvapil P, Otyepka M: **Environmental applications of chemically pure natural ferrihydrite**. *Environmental Science & Technology* 2007, **41**(12):4367–4374.

[8] Nosek J: **Laboratory research and modeling of nanoiron transport properties**. *Dissertation thesis*, Technical University of Liberec, Liberec, Czech Republic 2009.

[9] Pelikánová D: **Nanoparticle aggregation model**. *Diploma thesis*, Technical University of Liberec, Liberec, Czech Republic 2008.

[10] Somasundaran P, Runkana V: **Modeling flocculation of colloidal mineral suspensions using population balances**. *International Journal of Mineral Processing* 2003, **72**(1-4):33–55.

[11] Sun Y, Li Xq, Cao J, Zhang Wx, Wang HP: **Characterization of zero-valent iron nanoparticles**. *Advances in Colloid and Interface Science* 2006, **120**(1-3):47–56.

[12] Horak D, Petrovsky E, Kapicka A, Frederichs T: **Synthesis and characterization of magnetic poly(glycidyl methacrylate) microspheres**. *Journal of Magnetism and Magnetic Materials* 2007, **311**(2):500–506.

[13] Masheva V, Grigorova M, Nihtianova D, Schmidt JE, Mikhov M: **Magnetization processes of small gamma-Fe_2O_3 particles in non-magnetic matrix**. *Journal of Physics D: Applied Physics* 1999, **32**(14):1595–1599.

[14] Phenrat T, Saleh N, Sirk K, Tilton RD, Lowry GV: **Aggregation and sedimentation of aqueous nanoscale zerovalent iron dispersions**. *Environmental Science & Technology* 2007, **41**:284–290.

[15] Wang J, Wei LM, Liu P, Wei H, Zhang YF: **Synthesis of Ni nanowires via a hydrazine reduction route in aqueous ethanol solutions assisted by external magnetic fields**. *NanoMicro Letters* 2010, **1**:49–52.

[16] Gelbard F, Tambour Y, Seinfeld JH: **Sectional representations for simulating aerosol dynamics**. *Journal of Colloid and Interface Science* 1980, **76**(2):541–556.

[17] Elliott D, Li X, Zhang W: **Zero-valent Iron Nanoparticles for Abatement of Environmental Pollutants**. In *Particulate Systems in Nano- and Biotechnologies*. Edited by Ei-Shall H, Shah D, Sigmund W, Moudgil B, CRC Press 2008:309–329.

[18] Chuang FW, Larson RA, Wessman MS: **Zero-Valent Iron-Promoted Dechlorination of Polychlorinated Biphenyls**. *Environmental Science & Technology* 1995, **29**(9):2460–2463.

[19] Hou M, Wan H, Zhou Q, Liu X, Luo W, Fan Y: **The Dechlorination of Pentachlorophenol by Zerovalent Iron in Presence of Carboxylic Acids**. *Bulletin of Environmental Contamination and Toxicology* 2009, **82**(2):137–144.

[20] Lackovic JA, Nikolaidis NP, Dobbs GM: **Inorganic Arsenic Removal by Zero-Valent Iron**. *Environmental Engineering Science* 2000, **17**:29–39.

[21] Kanel SR, Greneche JM, Choi H: **Arsenic(V) removal from groundwater using nano scale zero-valent iron as a colloidal reactive barrier material**. *Environmental Science & Technology* 2006, **40**(6):2045–2050.

[22] Yuvakkumar R, Elango V, Rajendran V, Kannan N: **Preparation and characterization of zero valent iron nanoparticles**. *Digest Journal of Nanomaterials and Biostructures* 2011, **6**(4):1771–1776.

[23] Çelebi O, Üzüm c, Shahwan T, Erten H: **A radiotracer study of the adsorption behavior of aqueous Ba^{2+} ions on nanoparticles of zero-valent iron**. *Journal of Hazardous Materials* 2007, **148**(3):761–767.

[24] Ponder SM, Darab JG, Mallouk TE: **Remediation of Cr(VI) and Pb(II) Aqueous Solutions Using Supported, Nanoscale Zero-valent Iron**. *Environmental Science & Technology* 2000, **34**(12):2564–2569.

[25] Varanasi P, Fullana A, Sidhu S: **Remediation of PCB contaminated soils using iron nano-particles**. *Chemosphere* 2007, **66**(6):1031–1038.

[26] Nutt MO, Hughes JB, Michael SW: **Designing Pd-on-Au bimetallic nanoparticle catalysts for trichloroethene hydrodechlorination**. *Environmental science & technology* 2005, **39**(5):1346–1353.

[27] Cao J, Elliott D, Zhang Wx: **Perchlorate Reduction by Nanoscale Iron Particles**. *Journal of Nanoparticle Research* 2005, **7**(4-5):499–506.

[28] Liu Y, Majetich SA, Tilton RD, Sholl DS, Lowry GV: **TCE Dechlorination Rates, Pathways, and Efficiency of Nanoscale Iron Particles with Different Properties**. *Environmental Science & Technology* 2005, **39**(5):1338–1345.

[29] Schrick B, Hydutsky BW, Blough JL, Mallouk TE: **Delivery Vehicles for Zerovalent Metal Nanoparticles in Soil and Groundwater**. *Chemistry of Materials* 2004, **16**(11):2187–2193.

[30] Reardon EJ, Fagan R, Vogan JL, Przepiora A: **Anaerobic Corrosion Reaction Kinetics of Nanosized Iron**. *Environmental Science & Technology* 2008, **42**(7):2420–2425.

[31] Kanel SR, Manning B, Charlet L, Choi H: **Removal of Arsenic(III) from Groundwater by Nanoscale Zero-Valent Iron**. *Environmental Science & Technology* 2005, **39**(5):1291–1298.

[32] Ramos MAV, Yan W, Li Xq, Koel BE, Zhang Wx: **Simultaneous Oxidation and Reduction of Arsenic by Zero-Valent Iron Nanoparticles: Understanding the Significance of the CoreShell Structure**. *The Journal of Physical Chemistry C* 2009, **113**(33):14591–14594.

[33] Garrick S, Zachariah M, Lehtinen K: **Modeling and simulation of nanoparticle coagulation in high reynolds number incompressible flows**. In *Proceeding of the National Conference of the Combustion Institute* 2001:2527.

[34] McCurrie RA: *Ferromagnetic materials: structure and properties*. London: Academic Press 1994.

[35] Votruba V, Muzikar C: *Teorie elektromagnetického pole*. Akademia Praha 1958.

[36] Sedlak B, Stoll I, Man O: *Elektřina a magnetismus*. Praha: Academia Karolinum 1993.

[37] Rosicka D, Sembera J: **Inclusion of electrostatic forces to assessment of rate of magnetic forces impact to iron nanoparticle aggregation**. In *Nanocon 2011*, Brno: TANGER 2011.